

# DEVELOPMENT OF THE ALUMINUM BEAM DUCT FOR THE ULTRA-LOW EMITTANCE LIGHT SOURCE

Gao-Yu Hsiung<sup>†</sup>, Chia-Mu Cheng, Shen-Nung Hsu, Hsin-Pai Hsueh, Yi-Chen Yang, June-Rong Chen<sup>1</sup>, NSRRC, Hsinchu, Taiwan

<sup>1</sup>also at National Tsing Hua University, Hsinchu, Taiwan

## Abstract

The future light source with ultra-low emittance, typically < 500 pm rad, requests the beam duct with inner aperture < 20 mm for the electron storage ring. Besides, the cross section of the beam duct must be kept smooth for lowering the impedance. The aluminum extruded beam duct of 10 mm inside and 1 ~ 2 m in length was developed for this purpose. The beam duct was machined in ethanol to obtain a clean surface for a lower thermal outgassing rate. To mitigate the impedance of the flange connection, a special designed diamond-edge gasket and the aluminum flange without knife edge were developed. The inner diameters of both flange and gasket, 10 mm, are the same as that of beam duct. The sealing of the gasket has been proved leak-tight. The ultimate pressure and the thermal outgassing rate of the beam duct has achieved  $2 \times 10^{-10}$  Torr and  $1.4 \times 10^{-13}$  Torr l/(s cm<sup>2</sup>), respectively after baking. Those results fulfill both the ultrahigh vacuum and lowest impedance are applicable for the next generation ultra-low emittance light sources.

## INTRODUCTION

The future light source with ultra-low emittance, typically < 500 pm rad, based on the Multi-Bend Achromatic (MBA) lattice has been planned as the new or upgrading projects in many light source facilities [1]. It has been verified by the successful commissioning of the MAX IV in Sweden since 2015 [2, 3]. Then the similar design was adopted by other projects, e.g. SIRIUS in Brazil [4] et al. Since the beam duct of inner aperture typically < 20 mm and getting smaller for the electron storage ring was considered, then it has challenged the technical design of the vacuum systems [5]. Although the NEG-coated copper tube was employed in the MAX IV [6], which reveals the distributed pumping inside the vacuum duct, however the impact to the beam from the resistive-wall impedance of the duct, the concentration of residual gases in the duct, the RF-contact bridge of the flanges, etc. becomes serious especially for the smaller aperture. In this study, the aluminum extruded beam ducts with inner diameter of 10 mm and lengths of 1 m and 2 m were developed for evaluating the vacuum outgassing rate and ultimate pressure without the NEG-coating. The concepts learned from the TPS in Taiwan [7] were employed in this study which include:

(1) Oil-free ethanol CNC machining for the aluminum duct and vacuum components to achieve the ultra-low thermal outgassing rate.

(2) Ozonized water cleaning for lowering the surface outgassing rate and the photon stimulated desorption.

(3) RF-contact bridges and the diamond edge sealing for the modified flanges of beam ducts to minimize the coupling impedance.

The concepts of design, preparation of the beam ducts, experimental results, and the conclusions, will be addressed in the following sections.

## CONCEPTS OF DESIGN

Typically, the distance between the discrete vacuum pumps in the storage ring is about 2 m to 4 m. Then the maximum pressure inside the beam duct is located near the center about 1 m and 2 m, respectively, away from the pumps at the ends of ducts. It is equivalent to the pressure at the end of a long tube with lengths (L) of 1 m and 2 m, respectively. The maximum pressure can be calculated from the simple model of the pressure distribution for a long pipe [8].

$$P_L = q_D A \left( \frac{1}{S_P} + \frac{1}{2C} \right) = P_0 + \frac{q_D A}{2C} \quad (1)$$

where  $P_L$  and  $P_0$  are the pressures at the end and at the pump of the pipe, length = L, respectively. The  $q_D$  and A indicate the thermal outgassing rate and total surface-area of pipe, respectively. The  $S_P$  is the speed of the pump. The C is the conductance of the pipe can be calculated by [8]:

$$C = 12.1 \left( \frac{D^3}{L} \right) \quad (2)$$

where D is the inner diameter of the cylindrical long pipe. The vacuum parameters of the 1 m duct and 2 m duct for this study are listed in Table 1. If the maximum pressure ( $P_L$ ) of the pipe under the criteria of ultrahigh vacuum is <  $1 \times 10^{-9}$  Torr ( $1.33 \times 10^{-7}$  Pa), then the thermal outgassing rate ( $q_D$ ) must be lower than  $7.5 \times 10^{-13}$  and  $2.0 \times 10^{-13}$  Torr l/(s cm<sup>2</sup>) for 1 m and 2 m pipes, respectively.

Table 1: Vacuum Parameters of 1m Duct and 2 m Duct

Parameters	1 m duct	2 m duct
Length (L)	1 m	2 m
Inner diameter (D)	10 mm	10 mm
Conductance (C)	0.12 l/s	0.06 l/s
Surface-Area (A)	314 cm <sup>2</sup>	628 cm <sup>2</sup>
Max. Pressure ( $P_L$ )	< $1 \times 10^{-9}$ Torr	< $1 \times 10^{-9}$ Torr
Thermal Outgassing Rate ( $q_D$ )	< $7.5 \times 10^{-13}$ Torr l/(s cm <sup>2</sup> )	< $2.0 \times 10^{-13}$ Torr l/(s cm <sup>2</sup> )

Simulation of the pressure distribution for the 2 m long pipe, as shown in Fig. 1, at 4 cases of thermal outgassing rate ( $q_D$ ) that illustrates the criteria of  $q_D < 2.0 \times 10^{-13}$  Torr

<sup>†</sup> email address: hsiung@nsrrc.org.tw

Content from this work may be used under the terms of the CC BY 3.0 licence (© 2018). Any distribution of this work must maintain attribution to the author(s), title of the work, publisher, and DOI.

l/(s cm<sup>2</sup>), the curves (c) and (d), is required if pressure in the pipe <math>1 \times 10^{-9}</math> Torr.

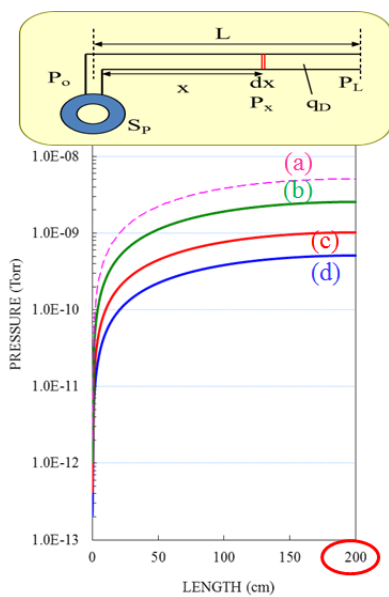


Figure 1: Simulation of the pressure distribution [8] in the 2 m long pipe, where  $q_D =$  (a)  $1.0 \times 10^{-12}$ , (b)  $5.0 \times 10^{-13}$ , (c)  $2.0 \times 10^{-13}$ , (d)  $1.0 \times 10^{-13}$  Torr l/(s cm<sup>2</sup>), respectively.

## EXPERIMENTAL

The aluminum extruded beam duct was selected for the reasons of high thermal conductivity, easier machining, and commercial availability. Preparation of the beam ducts and the experimental systems are described in the following sections.

### Preparation of the Beam Ducts

The commercial extruded A6063T5 aluminum (Al-) pipe, with inner diameter of 9.6 mm and outer diameter of 15.7 mm, was selected as the test beam ducts. The end flanges were made of A6061T651 aluminum alloys and machined the neck with same dimension as the tube for the welding purpose and the flange without knife edge, named the 16 DEF-flange in this study, for accommodating a special designed aluminum diamond edge (DE-) gasket sealing. The DE-gasket was made of the A1050O aluminum alloy, a soft material, for the vacuum sealing between the DEF-flanges via squashing the knife edges. The assembly drawings of the DEF-flanges and the DE-gasket are shown in Fig. 2. The Al-pipe of 1 m long was chemical cleaned prior to the welding of flanges. The TIG-welding was employed and confirmed the full penetration of the welding bead. Afterwards, the duct was removed for machining the inner surface by deep-drilling with a 1 m long drilling tool of 10 mm diameter penetrating through the duct including the flanges, flushing with ethanol, to enlarge the inner diameter overall from 9.6 mm to 10 mm as well as to form a fresh surface oxide layer. The animation of the deep drilling process and the photographs of the beam duct are illustrated in Fig. 3 and Fig. 4, respectively. For the 2 m beam duct, the Al-pipe was temporary cleaned up the end ports

for welding the Al DEF-flanges and then moved for deep drilling the inner surface to obtain a clean surface and 10 mm inner diameter.

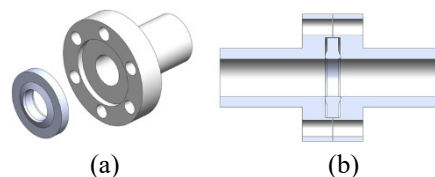


Figure 2: Assembly drawings of the DEF-flanges and the DE-gasket: (a) DE-gasket and DEF-flange, (b) cross section view of the DEF-flanges with DE-gasket sealing.

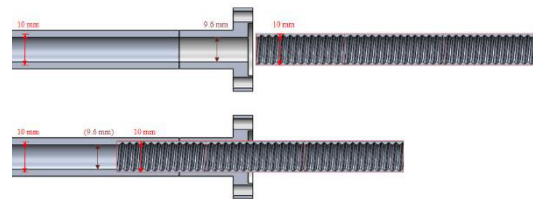


Figure 3: Animation of the deep drilling process for the beam duct to enlarge the inner diameter from 9.6 mm to 10 mm.

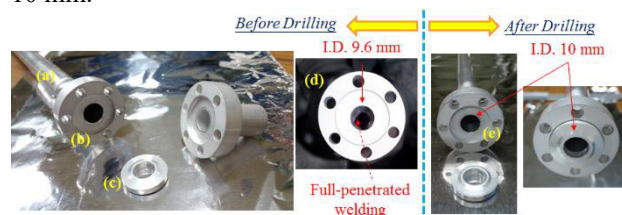


Figure 4: Photographs of the DEF-flanges and DE-Gasket for the beam duct: (a) Al-extruded pipe, (b) DEF-flange, (c) DE-Gasket, (d) Full-penetrated welding, (e) beam duct after oil-free deep-drilling process.

### Experimental Systems

The three experimental systems for the pumping measurements are shown in Fig. 5. The 1 m long beam duct was assembled as shown in Fig. 5(a) to measure the thermal outgassing rate via the throughput method. Afterwards, the 1 m beam duct was re-assembled as shown in Fig. 5(b) to directly pump down and measure the ultimate pressure as well as the thermal outgassing rate ( $q_D$ ) obtained from the Eq. (1). The similar process was applied to the 2 m beam duct assembled as shown in Fig. 5(c).

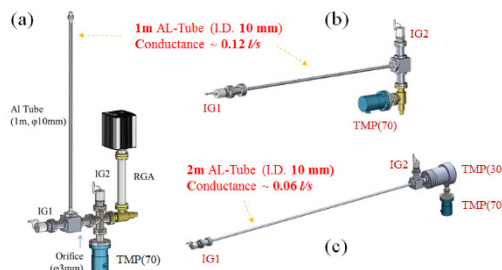


Figure 5: Assembly drawings of the experimental systems for 1 m duct in (a), (b), and for 2 m duct in (c).

In Fig. 5(a), there is an orifice of 3 mm in diameter installed between IG1 and IG2, IG represents the extractor ionization gauge, where IG1 measured the pressure (P1) of

outgas from 1 m beam duct and IG2 measured the pressure (P2) near the pump (TMP). The thermal outgas rate ( $q_0$ ) of the beam duct was obtained by the throughput method depicted by the following equation,

$$q_0 = C_0(P1 - P2)/A \quad (3)$$

where  $C_0 = 0.82$  l/s is the conductance of the orifice, and  $A$  is the surface area of the beam duct.

Each experimental systems were pumped down and vacuum baked to 150 °C for 1~3 days upon the various situations of slow-pumping feature that the pressure never exceeded the upper limit of  $1 \times 10^{-4}$  Torr through the baking period.

## Results

The measured thermal outgassing rates ( $q$ ) of the three experimental systems (a), (b), and (c), are illustrated as the curves shown in Fig. 6. The ultimate pressures and the thermal outgassing rates ( $q$ ) after baking are summarized in Table 2. The  $q$  values after baking were  $1.4 \times 10^{-13}$  and  $2.9 \times 10^{-13}$  Torr l/(s cm<sup>2</sup>) for 1 m and 2 m beam ducts, respectively. Figure 7 shows the photograph of the experimental system of AL(b)-1m in which the ultimate pressure of IG1 =  $6.06 \times 10^{-10}$  Torr (at the end) and IG2 =  $2.12 \times 10^{-10}$  Torr (near the pump) that demonstrates the ultrahigh vacuum performance after baking has been achieved. However, the pressure IG2 =  $1.8 \times 10^{-9}$  Torr for 2 m duct has not reached to the goal though the thermal outgassing rate was approaching to the criteria.

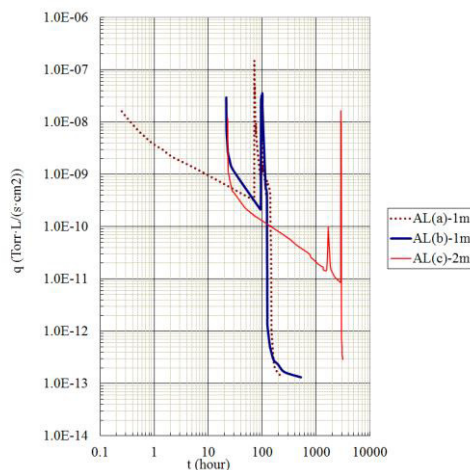


Figure 6: Curves of the thermal outgassing rates represented AL(a), AL(b) for 1 m duct, and AL(c) for 2 m duct.



Figure 7: Photograph of the experimental system for the 1 m beam duct of AL(b).

Table 2: Summary of Data

Ultimate Data after Baking	Ultimate Pressure IG1 (Torr)	Ultimate Pressure IG2 (Torr)	Thermal Outgassing Rate (q) (Torr l/(s cm <sup>2</sup> ))
AL(a)-1m	$3.1 \times 10^{-10}$	$2.3 \times 10^{-10}$	$1.3 \times 10^{-13}$
AL(b)-1m	$6.1 \times 10^{-10}$	$2.1 \times 10^{-10}$	$1.4 \times 10^{-13}$
AL(c)-2m	$1.8 \times 10^{-9}$	$6.8 \times 10^{-11}$	$2.9 \times 10^{-13}$

## CONCLUSION

The 1 m aluminum beam ducts with interior ethanol machining provides a clean surface with ultra-low thermal outgassing rate  $< 2 \times 10^{-13}$  Torr l/(s cm<sup>2</sup>) that the UHV pressure under  $1 \times 10^{-9}$  Torr can be achieved. It is equivalent to the maximum pressure neat the center of a 2 m long beam duct. However, the results are slightly higher in case of the 2 m beam duct but can be improved by the further cleaning with the ozonized water. The new designed aluminum diamond-edge (DE-) gasket with the DEF-Flanges without knife-edge developed for the ultra-low impedance RF contact shielding has performed the UHV sealing quality. This study provides the criteria of UHV and the quality of the 2-4 m long aluminum beam ducts with small aperture of 10 mm cooperated with the diamond-edge gasket sealing can be applied for the next generation ultra-low emittance light sources.

## ACKNOWLEDGEMENT

The authors would like to thank to Mr. W. C. Wong of Sheng-Shin Precision Industrial Ltd. Co. for providing the high quality ethanol machining supports for this work.

## REFERENCES

- [1] R. Hettel, "Challenges in the design of diffraction-limited storage rings", in *Proc. IPAC'14*, Dresden, Germany, June 2014, paper MOXBA01, pp. 7-11.
- [2] M. Eriksson, *et al.*, "Commissioning of the MAX IV light source", in *Proc. IPAC'16*, Busan, Korea, May 2016, paper MOYAA01, pp. 11-15.
- [3] S.C. Leemann, M. Sjöström, Å. Andersson, "First optics and beam dynamics studies on the MAX IV 3 GeV storage ring", in *Proc. IPAC'17*, Copenhagen, Denmark, May 2017, paper WEPAB075, 2756-2759.
- [4] L. Liu and H. Westfahl Jr., in *Proc. IPAC'17*, Copenhagen, Denmark, May 2017, paper TUXA1, 1203-1208.
- [5] P. He, "Accelerator vacuum technology challenges for next generation synchrotron-light sources", in *Proc. IPAC'17*, Copenhagen, Denmark, May 2017, paper FRXAB1, 4830-4835.
- [6] E. Al-Dmour, M. Grabski, "The vacuum system of MAX IV storage rings: installation and conditioning", in *Proc. IPAC'17*, Copenhagen, Denmark, May 2017, paper WEPVA090, 3468-3470.
- [7] G. Y. Hsiung, *et al.*, "Vacuum systems for the TPS accelerator", *Vacuum*, vol. 121, pp. 245-249, 2015.
- [8] A. Roth, *Vacuum Technology*, 3rd Ed., Elsevier Science B.V., North Holland, 1990.